Processing, interpretation and modeling of seismic reflection data in the Molasse Basin of eastern Switzerland

By Martin Stäuble[1]) and O. Adrian Pfiffner[2])

ABSTRACT

Seismic reflection profiles crossing the Plateau Molasse, the Subalpine Molasse, and reaching into the Helvetic Nappes of eastern Switzerland have been reprocessed, interpreted and modeled. Final stacks and some migrated data are presented here. Foreward modeling with 2-D ray tracing is used to confirm the structural features interpreted from the seismic data.

The basin is characterized by southward increase in thickness of the Tertiary strata which is associated with on-lap structures. The Triassic-Middle Jurassic sediments thin southward and show a notable change in seismic character at the northern edge of the Alemannic land which might be due to Jurassic synsedimentary faulting. The Mesozoic strata are dipping at a shallow angle towards the south. An abrupt change to a steeper dip occurs at the southern end of the Plateau Molasse and is related to the northward pinch-out of the Lower Marine Molasse (UMM). Inversion of the thick UMM in the Neogene compression stage lead to the development of a classic triangle zone. Thrust faults within the Subalpine Molasse level out at depth according to the seismic data and are related to folding and thrusting on the northern flank of the Aar massif.

ZUSAMMENFASSUNG

Reflexionsseismische Profile der Ostschweiz von der mittelländischen Molasse bis in die helvetischen Decken wurden neu aufbereitet, interpretiert und modelliert. Stapelungen und Migration werden hier gezeigt. Anhand 2-D raytracing Modellierungen wurde die geologische Interpretation der Profile überprüft.

Im Molassebecken nimmt die Mächtigkeit der tertiären Sedimentabfolgen gegen Süden zu, während sie für die Schichtreihe des darunterliegenden Mesozoikums in gleicher Richtung abnimmt. Die Zunahme der Mächtigkeit der Molasseschichten steht im Zusammenhang mit on-lap Strukturen. Die unterschiedliche seismische Fazies des Mesozoikums könnte durch jurassische, synsedimentäre Bruchtektonik bedingt sein. Das Mesozoikum fällt flach nach Süden ein. Am Übergang zwischen mittelländischer und subalpiner Molasse wird das Südfallen abrupt versteilt. Diese Diskontinuität entspricht etwa der nördlichen Begrenzung des Beckens der Unteren Meeresmolasse (UMM). Inversion dieses UMM-Beckens anlässlich der tertiären Kompression führte zur Ausbildung einer klassischen «triangle zone»: nahe der heutigen Oberfläche entstand eine Steilzone, flankiert von nordvergenten Aufschiebungen in der subalpinen Molasse und einer südvergenten Aufschiebung («Randunterschiebung») in der aufgerichteten mittelländischen Molasse. Im tieferen Teil dieser Struktur wurde ein UMM-Paket in die mittelländische Molasse hineingepresst. Die Überschiebungen innerhalb der subalpinen Molasse werden den seismischen Daten zufolge in der Tiefe flach und dürften somit in Zusammenhang mit der Falten- und Überschiebungstektonik in der Nordabdachung des Aarmassivs stehen.

---

[1]) Institute of Geophysics, ETH-Zürich, 8093 Zürich, Switzerland.
[2]) Geological Institute, University of Bern, 3012 Bern, Switzerland.

Introduction

In 1986 the Swiss National Research Foundation acquired some 120 km of seismic reflection data as part of its program Nr. 20 (NFP 20). NFP 20 was designed as a multidisciplinary geoscientific program aimed at investigating the deep structure of the Alps (PFIFFNER et al. 1988, 1991, FREI et al. 1989). The recorded profile is located in the Central Alps of eastern Switzerland. To expand this data set northward (Fig. 1) into the Molasse Basin, the NFP 20 profile was exchanged with seismic data recorded for hydrocarbon exploration by the Schweizerische Erdöl AG (SEAG).

The northernmost end of these traded seismic lines lies close to the German-Swiss border, near lake Constance (Fig. 1); from there it extends southward, across the Plateau Molasse and the Subalpine Molasse and it terminates within the front of the Helvetic nappes of the Alps.

This paper describes the reprocessing, interpretation and modeling of these industry-type seismic lines.
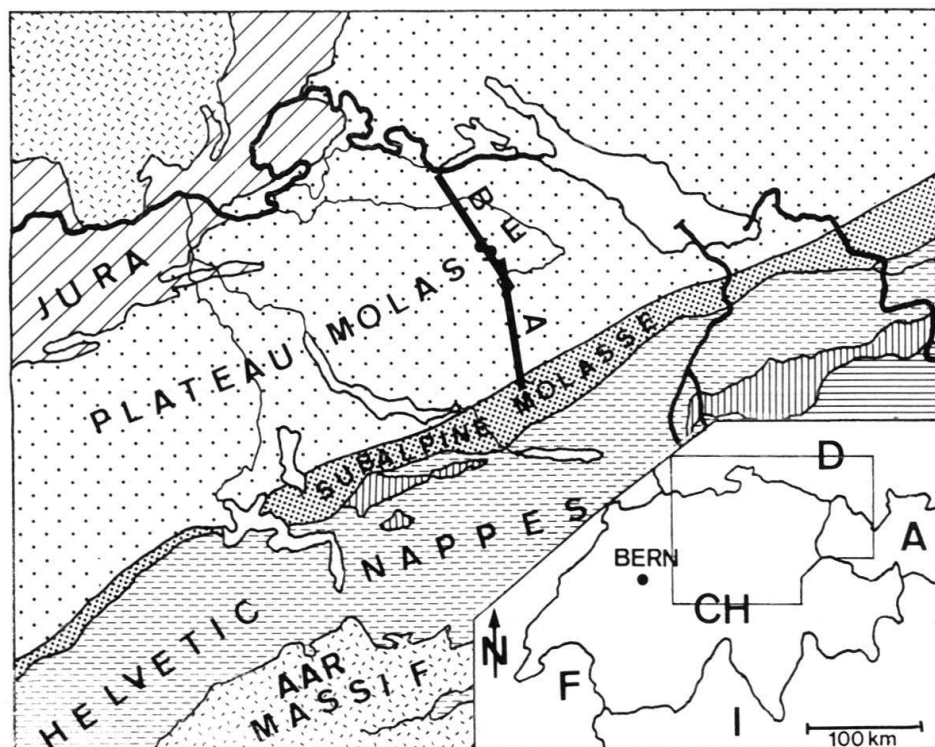
Fig. 1. Tectonic map of the Central Alps and their northern foreland, displaying the traces of the seismic sections.

Geological framework

The Molasse Basin (Fig. 1) can be separated into the essentially undeformed Plateau Molasse in the north (BÜCHI 1950, NAEF et al. 1985) and the imbricated Subalpine Molasse in the south (HABICHT 1945). The molasse sediments can be subdivided into four groups (Fig. 2). These are from top to bottom:

– The Middle Miocene OSM (Obere Süsswassermolasse, Upper Freshwater Molasse) consists of micaceous sandstones (Glimmersandstein, HOFMANN 1956) derived from the Austrian Alps and the Bohemian massif in a ENE-WSW direction, as well as conglomeratic fan deposits intercalated with shaly sandstones derived from the Alps in the south. Thickness of these fans varies between 1,500 m in the center of the gravel fans and a few 100 m in the north.

– The Early Miocene (Burdigalian) OMM (Obere Meeresmolasse, Upper Marine Molasse). It consists of mainly thick-bedded sandstones (FÜCHTBAUER 1967) and few conglomerates. Thickness increases from approximately 200 m in the north to 800 m in the south.

EPOCH / STAGE			MOLASSE GROUPS	LITHOLOGIES	THICK-NESS	AGE
					m	m.a.
TERTIARY	MIOCENE	SERAVALLIAN	Upper freshwater Molasse OSM	gravel fan deposits: mica-sandstones and conglomerates	~100 - 1500	11
		LANGHIAN				
		BURDIGALIAN	Upper marine Molasse OMM	sandstones	~200 - 800	20
		AQUITANIAN	Lower freshwater Molasse USM	gravel fan conglomerates	~4000	22
	OLIGOCENE	CHATTIAN				33
		RUPELIAN	Lower marine Molasse UMM	sandstones and shales	~1000	36
		SANNOISIAN				
	EOCENE				karst pockets	
	PALEOCENE			Bohnerz Fm		65
	CRETACEOUS		not deposited or eroded			135
MESOZOIC	JURASSIC	LATE JURASSIC	shaly limestones and limestones		~100	
		MIDDLE JURASSIC	shales, sandstones (and marls)		~50 - 50	
		EARLY JURASSIC	sandstones and shales		~50	195
	TRIASSIC	LATE TRIASSIC	shales and sandstones (anhydrite)		~50 - 100	
		MIDDLE TRIASSIC	dolomites, shales, sandstones (and anhydrite)		~50 - 200	
		EARLY TRIASSIC	not deposited or eroded			225
	BASEMENT		granites, gneisses permo-carboniferous sediments			

Fig. 2. Stratigraphic-lithologic overview of a complete section from the basement upward.

– The Late Oligocene to Early Miocene (Chattian-Aquitanian) USM (Untere Süss-wassermolasse, Lower Freshwater Molasse), contains sandstones and great masses of gravel fan conglomerates that were derived from the Alpine orogen. This clastic series reaches its greatest thickness of over 4 km in the Subalpine Molasse.

– The Early Oligocene (Rupelian) UMM (Untere Meeresmolasse, Lower Marine Molasse) is composed of shallow marine sandstones and shales (DIEM 1986). The sedimentation of the UMM was restricted to the southern part of the Molasse Basin, with outcrops found only in the Subalpine Molasse.

The molasse sediments overlie an 800 to 1,000 m thick sequence of Mesozoic sediments (BÜCHI 1965, LEMCKE 1961, 1968) which rest on the Variscan crystalline basement complex of the European crust. Regionally the basement is transected by a system of late Paleozoic grabens that are filled with Permo-Carboniferous, continental sediments (SPRECHER & MÜLLER 1986). In the area of the cross section under discussion (Fig. 1) no evidence for the occurrence of major Permo-Carboniferous grabens has been presented so far.

The base of the sequence (LEMCKE 1961, 1968) is formed by the Middle Triassic Lower Muschelkalk containing sandstones, followed by thin layers of anhydrite, shales and limestones (Fig. 2). These are capped by dolomites of the Upper Muschelkalk. From the Alpine thrust front the thickness of the Muschelkalk increases northward from approximately 50 m to over 200 m. The Upper Triassic Keuper consists of a sequence of shales and sandstones, interlaced with thin layers of anhydrite. The thickness of this unit decreases from approximately 100 m in the area of the lake Constance to less than 50 m near the Alpine deformation front. The Lower Jurassic is represented by sandstones and shales, less than 50 m thick, that thin out towards the Alpine belt. Shales, sandstones and marls are characteristic for the Middle Jurassic; their thickness ranges from approximately 150 m in the north to less than 50 m near the Alps. The Upper Jurassic consists of approximately 400–600 m thick shaly limestones (Oxfordian). The top of the Late Jurassic carbonate sequence corresponds to an erosional hiatus that developed during the Paleocene and Eocene. During this erosional phase Cretaceous and Jurassic sediments were eroded and carstified. Eocene lateritic deposits filling these karst pockets correspond to the Bohnerz formation.

The molasse sediments overlie more or less conformably the Mesozoic strata.

Data acquisition

The seismic reflection data were recorded for hydrocarbon exploration in the mid seventies (Fig. 1, line A, south) and the mid eighties (Fig. 1, line B, north). Fig. 3 shows the field parameters used for recording of the two lines. The differences in the recording parameters reflect the improvements made in acquisition from the 70s to the 80s. The advantage of the more modern recording technique and concept is apparent when comparing the northernmost profile B1 (Plate 4) and the southern profile A (Plate 1). In line B denser receiver and shot spacing, in combination with the higher frequencies resulted in better lateral and vertical resolution (SHERIFF 1977, YILMAZ 1987). In addition the use of combined Vibroseis and dynamite sources guaranteed a continuous subsurface coverage which provides an improvement in the signal-to-noise ratio. To ensure adequate source penetration with the relatively low fold (24) for the

	FIELD PARAMETERS	
LINE	**A**	**B**
RECORDING DATE	mid seventies	mid eighties
INSTRUMENT	DFS-V	SERCEL 348
SOURCE TYPE	VIBROSEIS (3 vibrators)	VIBROSEIS (3 vibrators) - DYNAMITE
GROUP INTERVAL	75 m	25 m
GROUP NUMBER	48 CHANNELS	120 CHANNELS
RECEIVER LAYOUT	100 m	25 m
SOURCE LAYOUT VIBROSEIS	30 m / 7m	10m 10m / 3m
SOURCE LAYOUT DYNAMITE	shot depth: 1.6-2 m / charge: (3-5) x 0.07 - 0.1 kg	●
SPREAD LAYOUT	1 48 / 412.5 m 3525 m	1 60 61 120 / 87.5m 87.5m / 1475 m 1475 m
SWEEP FREQUENCY	10 - 35 Hz	18 - 90 Hz
SWEEP LENGTH	14 s	7 s
SAMPLE INTERVAL	4 ms	2 ms
RECORD LENGTH	18 s	11 s
GAIN MODE	I.F.P	I.F.P
COVERAGE	24	60
FIELD FILTER	Low cut: OUT / High cut: 31 Hz	Low Cut: 12.5 Hz / High Cut: 72 Hz

Fig. 3. Field acquisition parameters of line A and B.

line A, each vibration point was vibrated 16 times, and subsequently vertically stacked in order to reduce random noise while increasing the signal strength by a factor of 4.

Processing

The processing center at the ETH Zürich was established by the NFP 20. It is based on a Vax-11/780 CPU with a MAP array processor subsystem and the Phoenix

processing package, a hardware/software configuration that was obtained from Seismograph Service Limited (SSL), London UK.

For both lines A and B a standard processing sequence (Fig. 4) was applied, resulting in both, final stacked sections (Plates 1, 3, 4 and 5) and migrated sections (Plate 2). No migration of line B is presented here.

The use of multiple energy sources in the line B resulted in a mixture of minimum phase traces from the dynamite source and zero phase traces from the Vibroseis source. When sorting the data from shot gathers into Common Depth Point (CDP) gathers, only traces with an identical phase should be present, otherwise the two different types of signal would cancel and degrade the subsequent stack. For this reason, the Vibroseis traces were converted to minimum phase. The operator was calculated from the autocorrelation of the sweep for line B and from sweep itself for line A. The conversion was also applied to line A although only Vibroseis was used as a source. This enabled the comparison of reflections from two different lines with the same phase characteristics.

In order to maximize subsurface resolution, the primary focus in processing was placed on velocity analysis in combination with residual statics calculation. Following filtering with deconvolution and bandpass, initial constant velocity stacks (CVA) of 25 CDP wide panels, every 100 CDP were calculated and analyzed to provide a first estimate of the normal moveout (NMO) correction. This provided a basis for a detailed mute analysis. The mute functions were then applied, prior to removing the initial
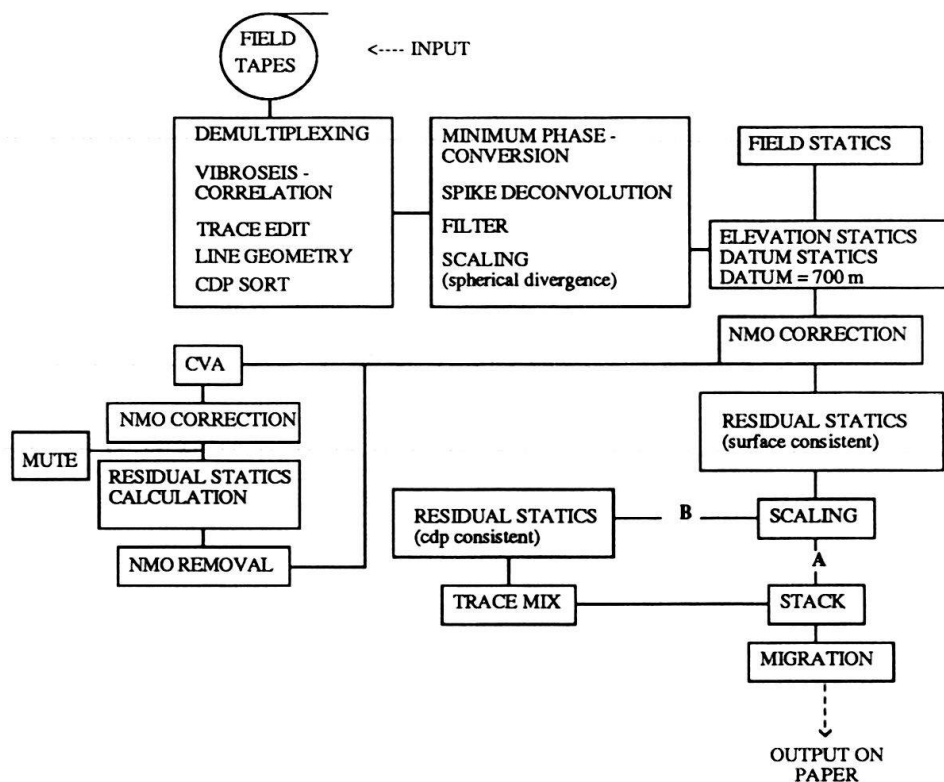

Fig. 4. Complete processing sequence applied to both data sets, with the iterative velocity-statics analysis displayed. Note the different steps applied to line B.

NMO correction. The resulting muted data set was then used for the first detailed CVA. After applying the NMO, initial surface consistent residual statics were calculated, applied, and NMO was again removed to recalculate a new CVA. This iterative process was repeated, until no further improvement was achieved. Initial filter parameters for deconvolution and band-pass filtering were reevaluated and optimized at this position in the processing sequence. For line A (Plate 1) this sequence produced an optimal stack. For line B (Plate 4) the stack could be improved by applying a CDP consistent statics (maximum shift allowed: 7 ms) followed by the mixing of the traces over a distance of 25 m.

For migration (FK-migration) the velocities were smoothed and reduced by 10% to reduce overestimation inherited from the 1-D assumption.

The seismic data

Plates 1, 2 and 3 give the stacked and migrated seismic sections for line A, and Plates 4 and 5 show the stacked data for line B. Because of confidentiality only a portion of line B is shown, whose position is indicated in the line drawing on Fig. 6a. In Plates 3 and 5 the interpretation is given directly on the stacked section. A summary of the more prominent reflectors is given to help improve the understanding of the line drawings (Figs. 5a and 6a) which do not depict the original "character" of the reflections. For the line drawings, reflections which were continuous for more than 10 CDPs (Line A = 375 m, line B = 250 m) were drawn, with the exception, where shorter reflections contributed to an obvious trend in coherency. In this sense the line drawings are the first interpretive step. The major reflections are labeled in the line drawing and are referred to in the following description. The most noticeable feature in line A (Plates 3 and 5) is the strong amplitude reflection band that occurs in the south at 3 s and that rises to 1.5 s at the northern end. This band, which contains several multicyclic reflections (Fig. 5a: a, b, c) is associated with the Mesozoic series overlying the basement. The strongest amplitude reflections at the top and the bottom of this band (Fig. 5a: a, c) can be traced confidently over the entire section. A strong reflection in the center of in this band (Fig. 5a: c), occurring in the north, weakens towards the south and becomes more difficult to trace. Faint reflections below the band occurring mainly between CDP 870 at 3 s two-way time (TWT) and CDP 600 at 3.3 s TWT are considered to be multiples from the above lying reflections and were excluded from the line drawing.

The Tertiary sedimentary sequence is characterized by good overall reflectivity, but only a few strong amplitude reflections (Fig. 5a: d, e, f) are traceable over more than 100 CDPs. Instead, this zone which extends from the surface down to approximately 2.5 s TWT in the south and 1.5 s TWT in the north, is dominated by short, discontinuous reflections. In the north the reflections are flat lying, changing to north plunging above 1.5 s at CDP 975 and south plunging at this point below 1.5 s. South of CDP 730 the dip changes abruptly to south dipping and flattens at 1.6 s between CDP 575 and 400. These reflections are cut off by steep, south-dipping reflections (Fig. 5a: g, h) reaching from CDP 600 at 0.25 s TWT down to 2 s TWT.

The sections displayed in Plates 4 and 5, called B1 and B2 are from the southern and central part of line B, respectively; their locations are given in the line drawing of

Fig. 6a. Section B2 is in part parallel to line A, but offset to the east by several kilometers (Fig. 1). A strong amplitude reflection band (Mesozoic) can be seen on B1 between 1 and 1.5 s TWT similar to line A, but it contains more fine, multicyclic reflections due to the higher frequency content of this section. Three strong reflections a, b and c in Fig. 6a are dominant in this band. A similar band occurs on section B2 between 1.3 and 1.8 s. TWT, with the top reflector appearing very weak. Above this band several strong, continuous, high frequency reflections within the Tertiary sequence are visible in panel B1 in d, e, f of Fig. 6a, but these are absent in panel B2. In panel B2, similar to section A, discontinuous reflections are characteristic.

Discussion

Lithologic interpretation

In order to interpret the reflection data, the section was converted from time to depth and the individual reflections were identified. Reflection identification is normally accomplished using synthetic seismograms derived from borehole measurements which then correlate with the surface recorded data. The lithologies of the wells drilled have been described in some detail (Büchi 1965). However, as the well data are only partially accessible to the public, a large part of our interpretation is based on surface extrapolations and ray tracing modeling (Fig. 7). As a consequence we cannot give a detailed lithological interpretation of the reflections, but concentrate on structural interpretation.

The velocities used for the depth conversion were in part taken from interval velocities and from published data (Lohr 1967). Interval velocities, calculated using the Dix equation (Yilmaz 1987) are considered to be reliable for the plane layering case. This is mostly true for the line B and the northern part of line A. For the Subalpine Molasse, velocities were interpolated from velocity studies in the Alps (Sellami et al. 1990, Stäuble et al. in press).

Reflection (f) is interpreted to originate from the top of the Upper Marine Molasse, i.e. the change from micaceous sandstones of the OSM to thick bedded marine sandstones of the OMM. The transition of the OMM sandstones to conglomerates of the USM is indicated by reflection (e). Reflection (d) is most likely the signature of beds of sandstones and conglomerates from within the USM. Although the lithological layering of the molasse sediments is expected to be highly reflective, the lack of traceable reflections to the south indicates that the reflectivity is more governed by the lateral discontinuity of the beds (Yilmaz 1987). The fresnel zone (limit of lateral resolution) is approximately 200 m for line B (at 0.5 s TWT, 4,000 m/s velocity and 50 Hz) and about 320 m (20 Hz) for line A.

The reflections from the top of the Mesozoic (a) are interpreted as stemming from the transition of the molasse sediments (sandstones and shales) to the carbonates of the Upper Jurassic, with the less reflective stretches (e.g. CDP 2,100–2,500 line B2) interpreted as being more karstic. Reflection (b) is associated with the change from Middle Jurassic sandstones to Upper Jurassic carbonates, and reflector (c) is identified as coming from the Late Triassic Keuper which contains beds of evaporites. The top basement is not identified as a strong reflection (Sprecher & Müller 1986), suggesting that this boundary lacks significant impedance contrast.
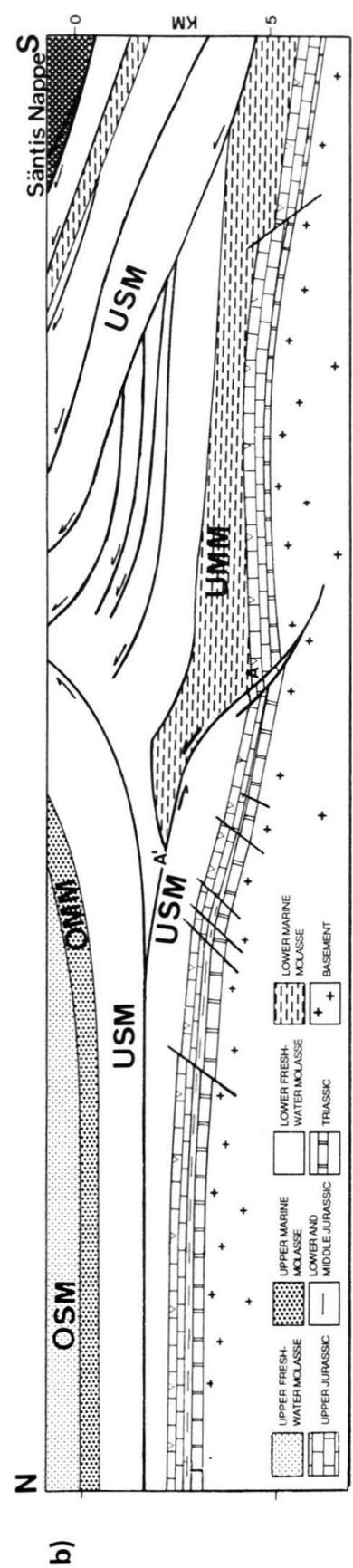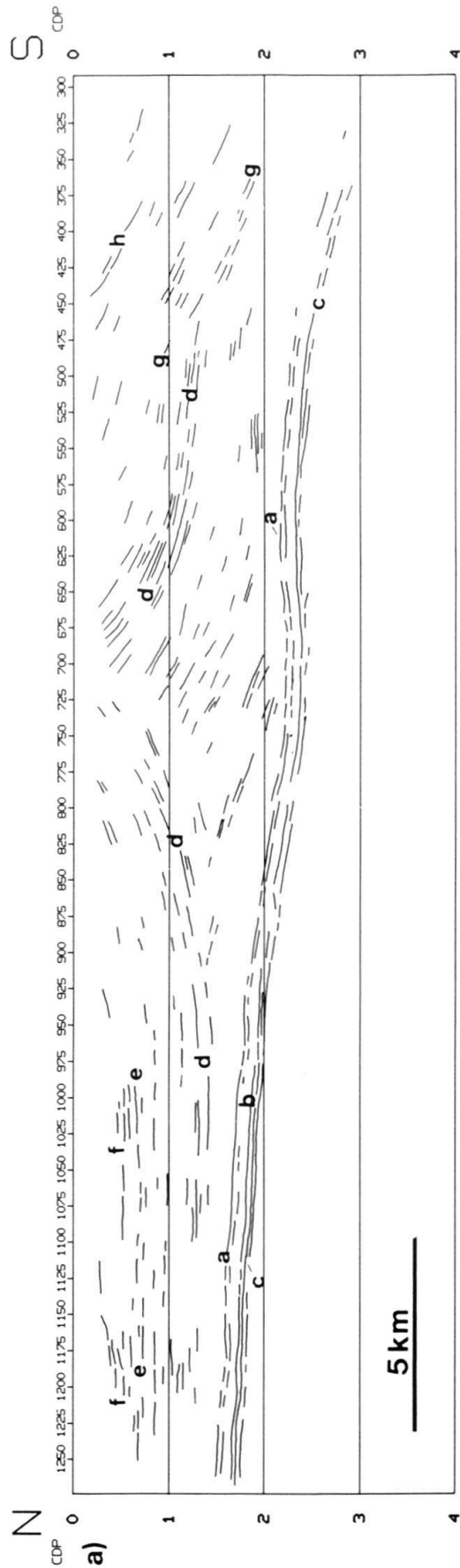
Fig. 5. a) Line drawing based on the stacked section A of Plates 1 and 2. Letters are reflections discussed in the text. b) Geologic interpretation of section A.
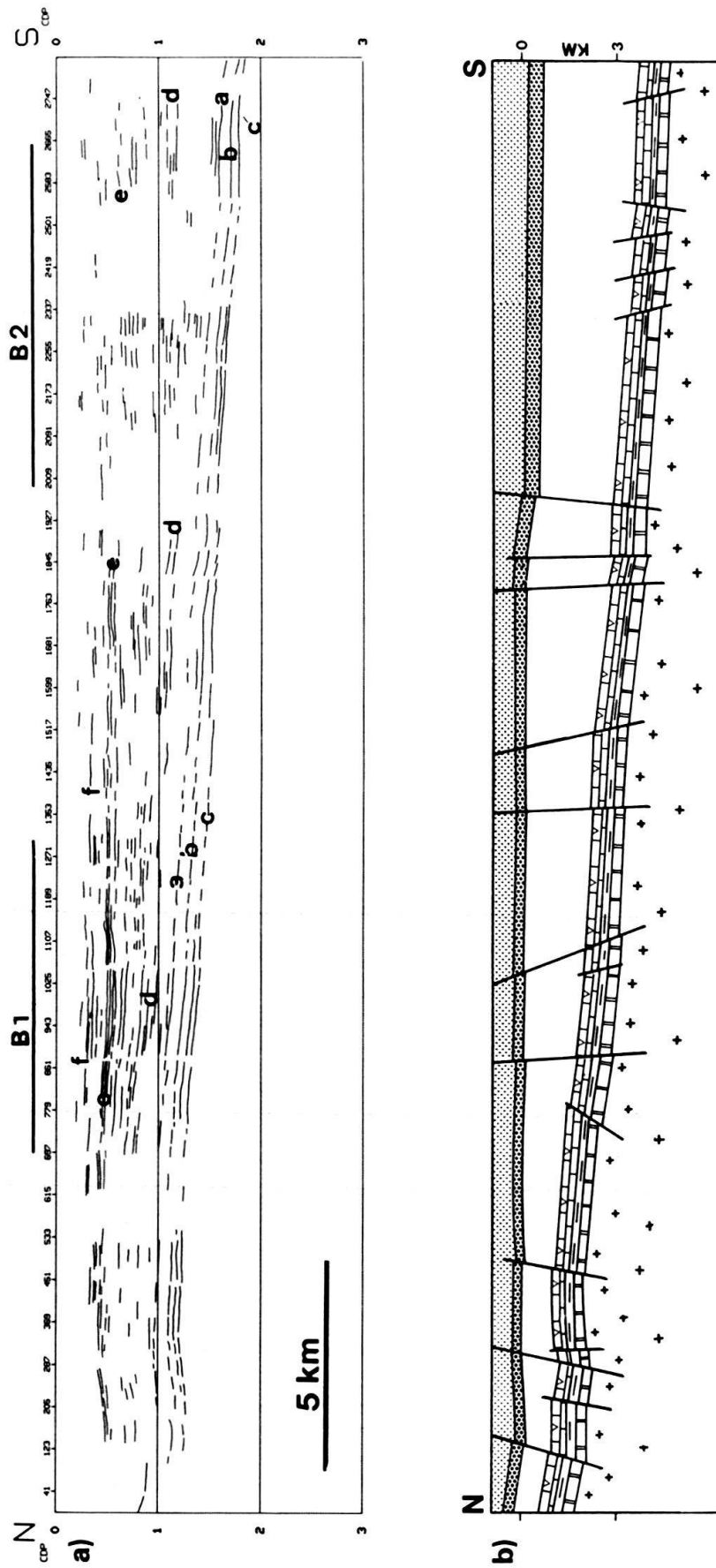
Fig. 6. a) Line drawing of the complete section B, with bars indicating the position of panels B1 and B2. b) Geologic interpretation of section B, using the same signatures as in Fig. 5b.

Structural interpretation

Figures 5b and 6b give the interpretation of the seismic sections. From north to south section B is characterized by high-angle normal faulting with apparent throws of up to 150 m. Some of them are restricted to the Mesozoic, while others dissect the entire sedimentary cover and thus are seemingly younger. The older faults restricted to the Mesozoic, are observed along the whole transect, whereas, the younger ones are only observed in the northern part of this line.

The Mesozoic is located at a depth of 1 km at the northernmost end of the section. It has a southward dip and thins continuously towards the south. The molasse sediments on the other hand thicken to the south. This is particularly evident for the USM. Onlap reflections are evident between Molasse and the top Mesozoic reflection (a) as well as within the molasse sediments themselves. The OMM and the OSM show only a moderate southward increase in thickness.

In section A, the Mesozoic continues dipping southwards, displaying several high-angle faults, all seemingly restricted to the Mesozoic sediments (Fig. 5). The Middle Jurassic (reflection b, Fig. 5) thins out to the south, leaving only two strong reflections from the top Jurassic (a) and Triassic (c) (Plates 1 and 3).

To the south the molasse sediments are tilted progressively into a steep northward dip, with south-dipping reflections branching off at CDP 850. At CDP 720 an abrupt change to a general southern dip of the whole molasse group occurs, which coincides with a zone of vertical bedding observed at the surface. This gives rise to a reflection configuration of a classic triangle zone. This triangle zone is interpreted as a wedge of UMM strata which was thrusted northward into the Plateau Molasse (Fig. 5b, A-A'), splitting it apart and rotating the beds above it into their present orientation. Similar structures are well documented in the Foothills of the Rocky Mountains of Alberta (BALLY et al. 1966, PRICE 1981) and have been used to interpret the tectonic style in the Molasse Basin of Bavaria (MÜLLER et al. 1988) located east of the study area. Outcrops of vertical USM beds, are found in the core of this triangle zone (see also HABICHT 1945) and they are flanked by dipping thrust faults with "top to the south" movements in the tilted Plateau Molasse (the "Randunterschiebung") and "top to the north" movements in the Subalpine Molasse. Further to the south, the more gently south dipping USM strata are repeated in several imbricate thrust sheets (reflections g and h) that involve also the UMM sediments (HABICHT 1945, PFIFFNER 1986). In the seismic section these faults can be traced to below 2 s TWT (or to depth greater than 5 km). The geometry of the Säntis thrust at the base of the Säntis Nappe shown in Fig. 5b at the southernmost tip of the section, is based on geologic observations, rather than on seismic reflections.

Modeling

As a verification of this interpretation, the triangle zone between the Plateau and the Subalpine Molasse was modeled by means of synthetic seismograms (Fig. 7), using a 2-D normal incidence ray tracing technique. In a stacked section, the traces represent coinciding source and receiver recording. This can be simulated by using normal incidence ray tracing. For model building and ray tracing, the SIERRA (a software
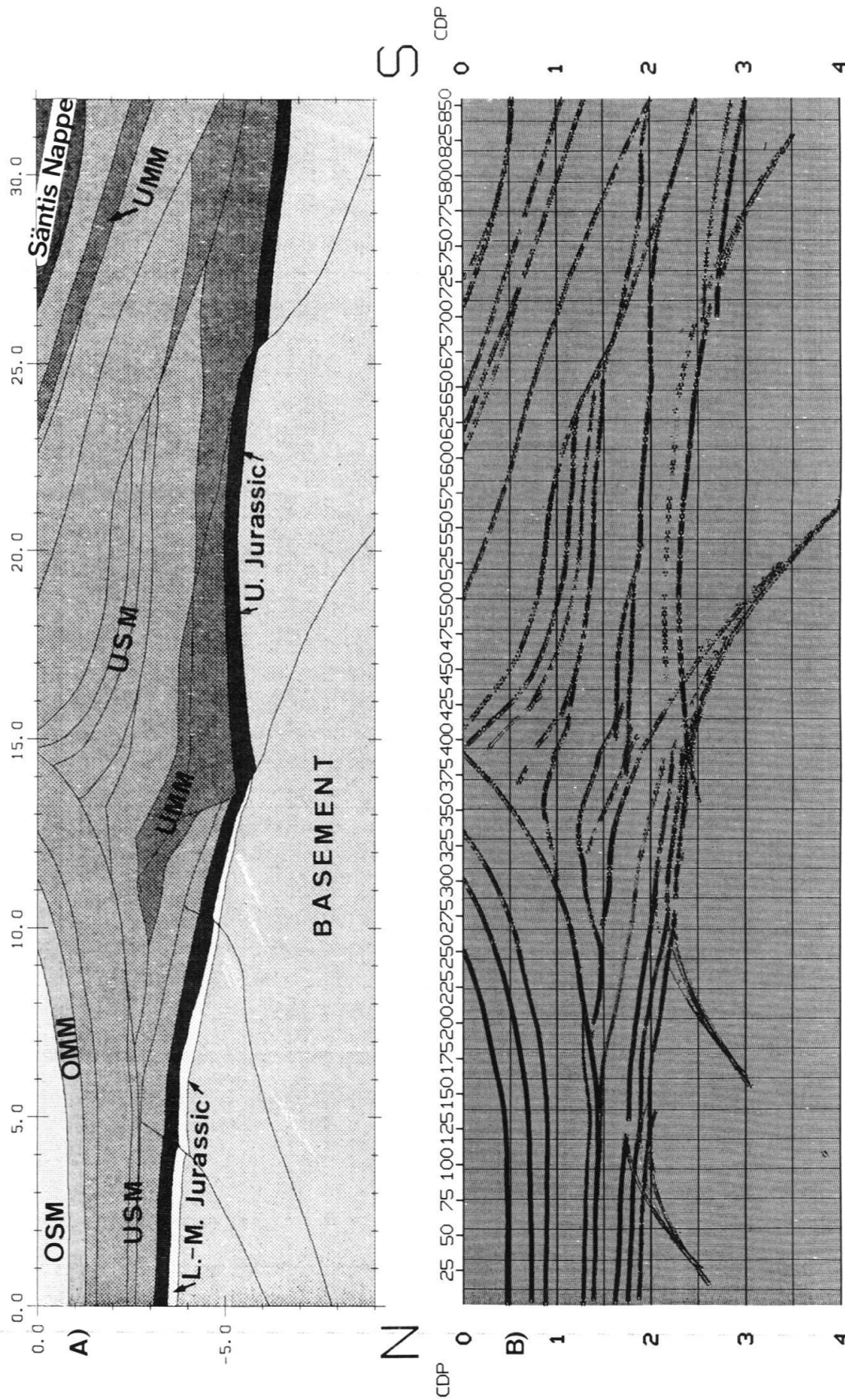
Fig. 7. A) Computer model of the triangle zone in section A. The layers are shaded according to the lithologies. B) Synthetic response of the model.

product of Sierra Geophysics Inc., Houston) 2-D and 3-D modeling program was used. An array of 37.5 m spaced coincident receiver and shot points was ray traced, resulting in a time-reflection coefficient series. These coefficient series were then convolved using a minimum-phase Ricker wavelet with a center frequency of 20 Hz to produce a synthetic seismogram. For a more detailed discussion of the modeling technique the reader is referred to Stäuble et al. (in press) and Litak et al. (in press). The synthetic seismogram was compared with the observed data, and where necessary, the model was improved until a satisfactory match between the observed data and the synthetic section was achieved. The corrections to the model were in structure, i.e. the position and the shape of the reflector were changed and not the velocities. In particular it concerned the exact position and shape of the UMM and the Mesozoic. To avoid scattering of rays on small undulations the surfaces were filtered to present a smooth surface. The final model consists of 38 layers (the dominant reflectors were modeled) which incorporates the same velocities used for the depth conversion. Within the area of the seismic profile the structures of the Molasse Basin are rather continuous along trend, therefore the 2-D modeling assumption is considered to be valid. The final model confirms the overall structural interpretation, but does not represent finer details. Incorporations of the nature of small-scale displacements and layering would not alter these results and would be beyond the capabilities of this technique.

Conclusions

In the transect of the seismic sections presented here the Molasse Basin is structurally characterized by vertical movements and considerable thrusting and folding in the Subalpine Molasse. Two phases of normal faulting can be distinguished. First a period of Mesozoic normal faulting is associated with the rise of the Alemannic land (Trümpy 1949) resulting in the downthrow of the northern block. During the Tertiary a second phase of normal faulting, was associated with strong subsidence downthrowing the southern block and marks the onset of sedimentation at the southernmost end of the Molasse foredeep. The earliest episodes of the Tertiary basin formation covers the deposition of the North-Helvetic Flysch and was followed by the accumulation of the UMM series (Pfiffner 1986). Synsedimentary normal faults controlled the geographic extension of certain formations. E.g. the northernmost limit of the Lower Marine Molasse sedimentation coincides with such a normal fault (Fig. 5b, A-A') of considerable throw. The extensional features of this second phase developed in a compressional regime of a collisional type orogeny. Downbending of the subducting European lithosphere (Laubscher 1978, Pfiffner 1986) resulted in extension at the outer arc of the bent slab, and caused the uplift of the Jura Plateau further to the north.

With continued, rapid subsidence the depocenter prograded out into the foreland, as indicated in the seismic section by several onlaps of molasse sediments onto the Mesozoic strata and onto the molasse sediments themselves. Some angular unconformities in the molasse sediments can be found at outcrop (Pavoni 1956).

In the northern part of the transect several normal faults dissect the whole molasse section and are thus of post Mid-Miocene age. As the Alpine thrusting migrated further into the foreland (Pfiffner 1986) an inversion of the preexisting faults (Fig. 5,

A-A') took place. Such inversions, as described in the western Alps by BUTLER (1989), result in vertical movements and steepening of the overlying beds. In the example of this transect the inversion is interpreted to be responsible for the formation of the triangle zone discussed earlier. The shortening represented by the imbricates of the UMM and the USM beds in the Subalpine Molasse is balanced by shortening in the basement south of the seismic section in the Aar Massif (PFIFFNER et al. in press, STÄUBLE et al. in press). From the seismic results it is not possible to connect thrusts from the Subalpine Molasse backward to the Glarus-Säntis thrust, a possibility evoked by Pfiffner (1986, solution 1). Instead all the thrusts of the Subalpine Molasse are likely to correspond to reflections reaching well below 2 s TWT, and thus seem to connect with the thrusts on the northern flank of the Aar Massif.

Acknowledgments

REFERENCES

BALLY, A.W., GORDY, P.L. & STEWART, G.A. 1966: Structure, seismic data and orogenic evolution of the southern Canadian Rocky Mountains. Bull. canad. Petroleum Geol. 14, 337–381.

BÜCHI, U.P. 1950: Zur Geologie und Paläogeographie der südlichen mittelländischen Molasse zwischen Toggenburg und Rheintal. PhD-Thesis, University of Zürich, Switzerland.

— 1965: Geologische Ergebnisse der Erdölexploration auf das Mesozoikum im Untergrund des schweizerischen Molassebeckens. Bull. Ver. schweizer. Petroleum-Geol. u. -Ing. 32, 7–38.

BUTLER, R.W.H. 1989: The influence of pre-existing basin structure on thrust system evolution in the Western Alps. In: Inversion Tectonics, Ed. by COOPER, M.A. & WILLIAMS, G.D., Geological Society Spec. Publ. 44, 105–122.

DIEM, B. 1986: Die Untere Meeresmolasse zwischen der Saane (Westschweiz) und der Ammer (Oberbayern). Eclogae Geol. Helv. 79, 493–559.

FREI, W., HEITZMANN, P., LEHNER, P., MÜLLER, ST., OLIVIER, R., PFIFFNER, O.A., STECK, A. & VALASEK, P. 1989: Geotraverses across the Swiss Alps. Nature 340, 544–548.

FÜCHTBAUER, H. 1967: Die Sandsteine in der Molasse nördlich der Alpen. Geol. Rdsch. 56, 266–300.

HABICHT, K. 1945: Geologische Untersuchungen im südlichen sanktgallisch-appenzellischen Molassegebiet. Beitr. Geol. Karte Schweiz. N.F. 83.

HOFMANN, F. 1956: Die Obere Süsswassermolasse in der Ostschweiz und im Hegau. Bull. Ver. schweizer. Petroleum-Geol. u. -Ing. 23, 23–34.

LEMCKE, K. 1961: Zur Kenntnis des vortertiären Untergrundes im Bodenseegebiet. Bull. Ver. schweizer. Petroleum-Geol. u. -Ing. 27, 9–14.

— 1968: Einige Ergebnisse der Erdölexploration auf die mittelländische Molasse der Zentralschweiz. Bull. Ver. schweizer. Petroleum-Geol. u. -Ing. 35, 15–34.

LAUBSCHER, H.P. 1987: Foreland folding. Tectonophysics 47, 325–337.

LOHR, J. 1967: Die seismischen Geschwindigkeiten der Ostschweiz. Bull. Ver. schweizer. Petroleum-Geol. u. -Ing. 34, 29–38.

MILNES, A.G. & PFIFFNER, O.A. 1980: Tectonic Evolution of the Central Alps in the cross section St. Gallen-Como. Eclogae geol. Helv. 73, 619–633.

MÜLLER, M., NIEBERDING, F. & WANNINGER, A. 1988: Tectonic style and pressure distribution at the northern margin of the Alps between Lake Constance and the River Inn. Geol. Rdsch. 77, 787–796.

NAEF, H., DIEBOLD, P. & SCHLANKE, S. 1985: Sedimentation und Tektonik im Tertiär der Nordschweiz. Nagra Tech. Ber. NTB 85-14. Nagra, Baden.
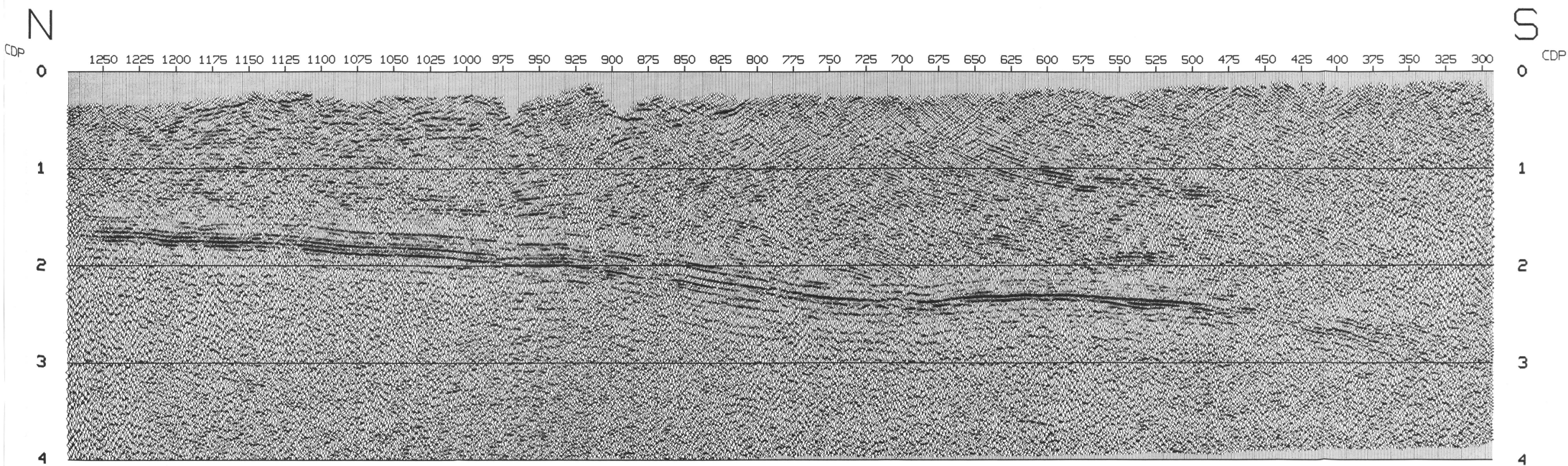
Pavoni, N. 1956: Zürcher Molasse und Obere Süsswassermolasse der Ostschweiz, ein stratigraphischer Vergleich. Bull. Ver. schweizer. Petroleum-Geol. u. -Ing. 22, 25–32.

Pfiffner, O.A. 1986: Evolution of the north Alpine foreland basin in the Central Alps. In: Foreland basins, Ed. by Allen, P.A. & Homewood, P. Int. Assoc. Sedimentol., Spec. Publ. 8, 219–228.

Pfiffner, O.A., Frei, W., Finck, P. & Valasek, P. 1988: Deep seismic reflection profiling in the Swiss Alps: Explosion seismology results for the line NFP 20-East, Geology 16, 987–990.

Pfiffner, O.A., Klaper, E.M., Mayerat, A.-M. & Heitzmann, P. 1990: Structure of the basement-cover-contact in the Swiss Alps. In: Deep structure of the Alps, Ed. by Roure, F., Heitzmann, P. & Polino, R. Mém. Soc. Géol. France 156.

Pfiffner, O.A., Frei, W., Valasek, P., Stäuble, M.P., Levato, L., DuBois, L., Schmid, S.M. & Smithson, S.B. 1990: Crustal shortening in the Alpine orogen: results from the deep seismic reflection profiling in the eastern Swiss Alps, line NFP 20-East. Tectonics 9, 1327–1355.

Price, R.A. 1981: The Cordilleran foreland thrust and fold belt in the southern Canadian Rocky Mountains. In: Thrust and Nappe tectonics, Ed. by McClay, K.R. & Price, N.J. Geol. Soc. London, Spec. Publ. 9, 427–448.

Sellami, S., Barblan, F., Mayerat, A.-M., Pfiffner, O.A., Risnes, K. & Wagner, J.J. 1990: Compressional wave velocities of samples. In: Deep structure of the Alps, Ed. by Roure, F., Heitzmann, P. & Polino, R. Mém. Soc. Géol. France 156.

Sheriff, R.E. 1977: Limitations on resolution of seismic reflections and geologic detail derivable from them. In: Seismic stratigraphy – Application to hydrocarbon exploration, Ed. by Payton, C.E. Am. Ass. Petr. Geol. Mem. 26, 3–14.

Sprecher, Ch., Müller, W.H. 1986: Geophysikalisches Untersuchungsprogramm Nordschweiz: Reflexionsseismik 82. Nagra Tech. Ber. NTB 84-15. Nagra, Baden.

Stäuble, M.P. & Pfiffner, O.A. (in press): Evaluation of the seismic response of basement thrust and fold geometry in the Central Alps based on 2-D ray tracing. Ann. Tect.

Stäuble, M.P., Smithson, S. & Pfiffner, O.A. (in press): Interpretation of reflection profiles in the Eastern Swiss Alps based on 3-D Raytracing modeling. Tectonics.

Trümpy, R. 1949: Der Lias der Glarner Alpen. Mitt. geol. Inst. ETH u. Univ. Zürich, Serie C, 36, and Denkschr. schweiz. natf. Ges. 79/1.

—   1980: Geology of Switzerland, a guide book. Schweiz. Geol. Komm., Basel, New York: Wepf & Co. Publ.

Yilmaz, Ö. 1987: Investigations in Geophysics No. 2: Seismic data processing. Soc. of Exploration Geophys.

Plate 1

Stacked section of line A. Displayed with AGC = 500 ms, Scale = 1:75,000, compression black.

N
S

CDP

N: 1250 1225 1200 1175 1150 1125 1100 1075 1050 1025 1000 975 950 925 900 875 850 825 800 775 750 725 700 675 650 625 600 575 550 525 500 475 450 425 400 375 350 325 300 : S
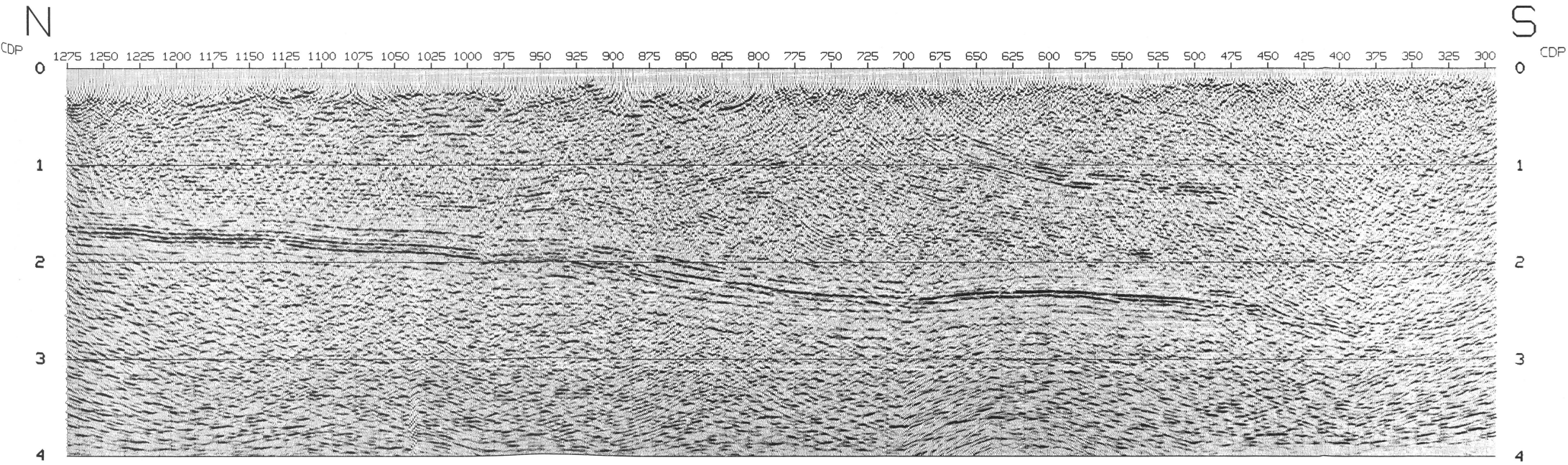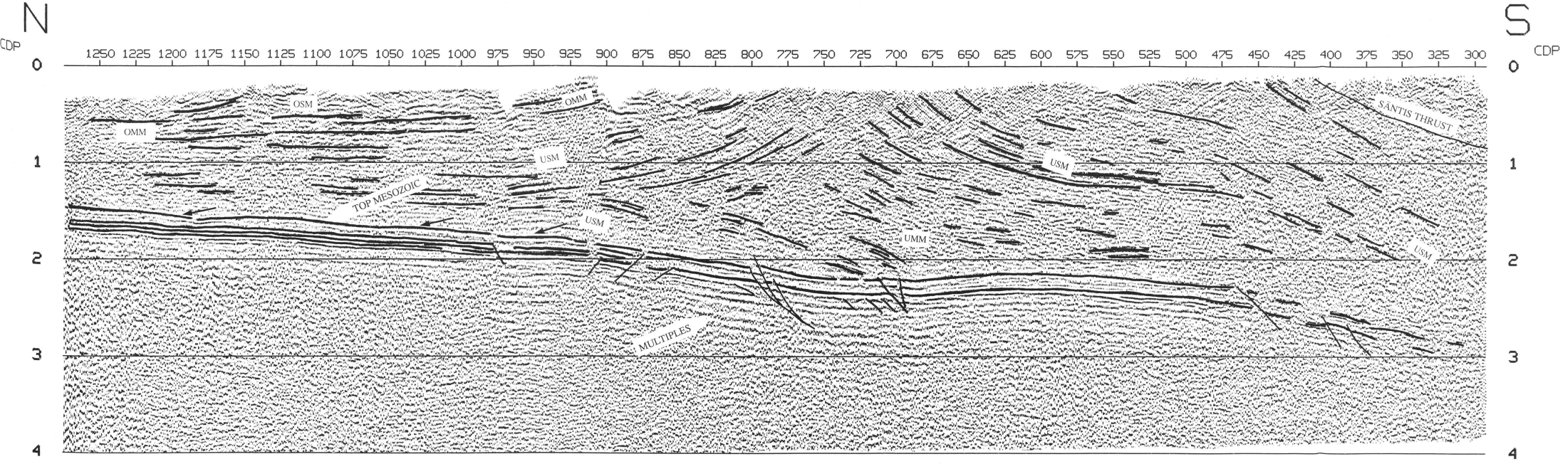
CDP

Plate 2

Migrated section A. FK-migration using smoothed velocity functions, reduced by 10%.

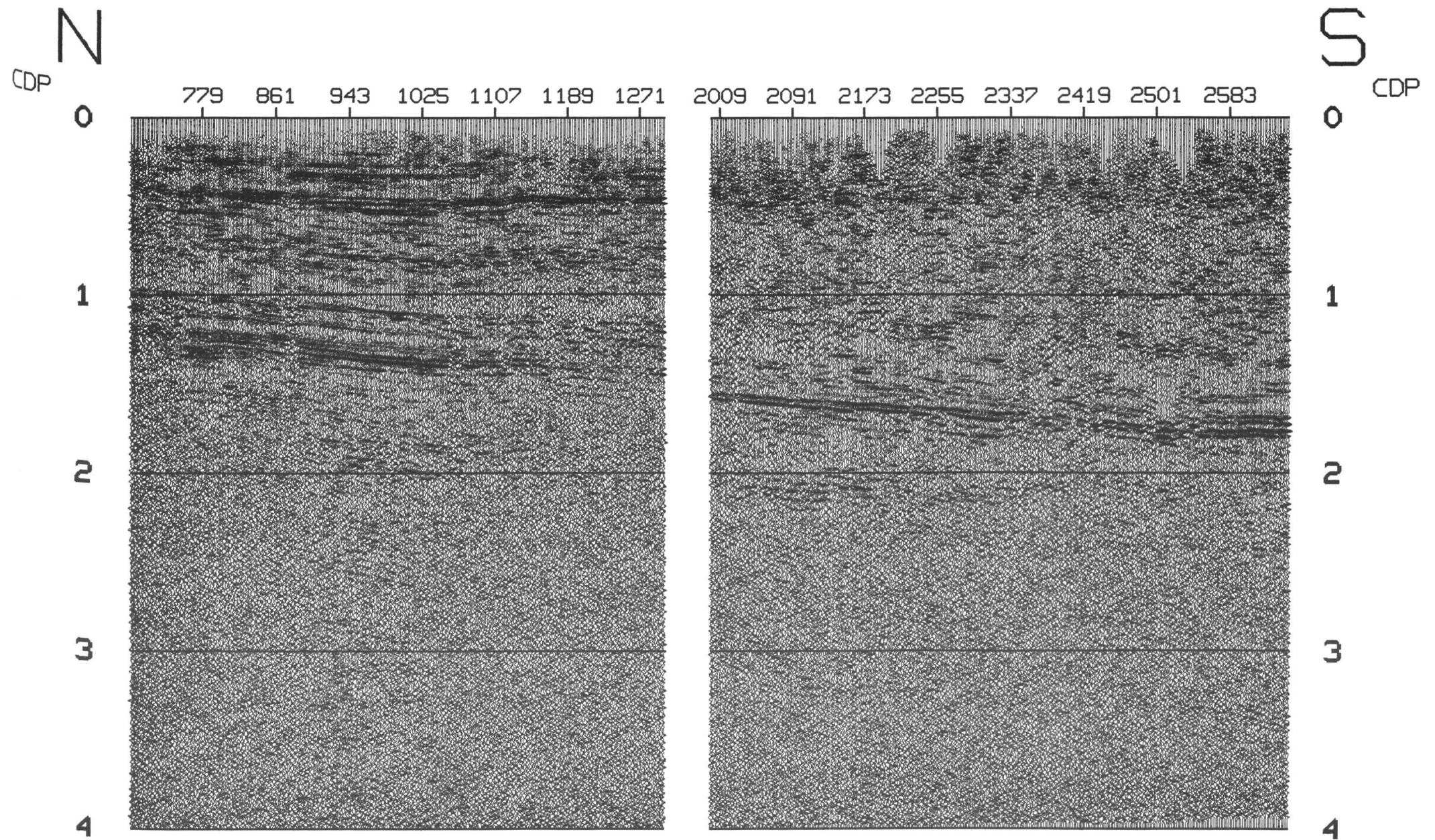## Plate 3

The same section as Plate 1 with only the positive amplitude area plotted and enhanced by line drawings. Onlaps are indicated with arrows.

Plate 4

Panels B1 and B2 of section B, stacked. The exact position of B1 and B2 is given in Fig. 6a. Displayed with AGC = 500 ms, compression = black, scale = 1:75,000, 1:1 with a constant velocity of 5 km/s.

Plate 5

The same section as Plate 4, with only the positive amplitude area plotted and enhanced by line drawings. Onlaps are indicated with arrows.